

Geophysical Research Letters



RESEARCH LETTER

10.1029/2018GL081625

Key Points:

- Diurnal variations of turbulent heat fluxes are well estimated by the maximum power limit for sites with contrasting land cover in Amazonia
- Land cover affected primarily the absorption of solar radiation and the partitioning of turbulent fluxes into sensible and latent heat
- Thermodynamic theory is well suited as a parsimonious approach to describe first-order controls of land-atmosphere interactions

Supporting Information:

- Supporting Information S1

Correspondence to:

L. Conte and A. Kleidon,
giggi.conte@gmail.com;
akleidon@bgc-jena.mpg.de

Citation:

Conte, L., Renner, M., Brando, P., Oliveira dos Santos, C., Silvério, D., Kolle, O., et al. (2019). Effects of tropical deforestation on surface energy balance partitioning in southeastern Amazonia estimated from maximum convective power. *Geophysical Research Letters*, *46*, 4396–4403. <https://doi.org/10.1029/2018GL081625>

Received 8 DEC 2018

Accepted 29 MAR 2019

Accepted article online 3 APR 2019

Published online 22 APR 2019

©2019. The Authors.

This is an open access article under the terms of the Creative Commons Attribution-NonCommercial-NoDerivs License, which permits use and distribution in any medium, provided the original work is properly cited, the use is non-commercial and no modifications or adaptations are made.

Effects of Tropical Deforestation on Surface Energy Balance Partitioning in Southeastern Amazonia Estimated From Maximum Convective Power

Luigi Conte¹ , Maik Renner¹ , Paulo Brando^{2,3}, Claudinei Oliveira dos Santos², Divino Silvério² , Olaf Kolle¹ , Susan E. Trumbore¹ , and Axel Kleidon¹ 

¹Max Planck Institute for Biogeochemistry, Jena, Germany, ²Instituto de Pesquisa Ambiental da Amazônia, Brasília, Brazil, ³Woods Hole Research Center, Falmouth, MA, USA

Abstract To understand changes in land surface energy balance partitioning due to tropical deforestation, we use a physically based analytical formulation of the surface energy balance. Turbulent heat fluxes are constrained by the thermodynamic maximum power limit and a formulation for diurnal heat redistribution within the land-atmosphere system. The derived turbulent fluxes of sensible and latent heat compare very well to in situ observations for sites with intact rainforest and soybean land cover in southeastern Amazonia. The equilibrium partitioning into sensible and latent heat flux compares well with observations for both sites, except for the soybean site during the dry season where water limitation needs to be explicitly accounted for. Our results show that tropical deforestation primarily affects the absorption of solar radiation and the water limitation of evapotranspiration, but not the overall magnitude of turbulent heat fluxes that is set by the thermodynamic maximum power limit.

Plain Language Summary Tropical deforestation impacts the local energy and water exchange between land surface and atmosphere, typically resulting in regionally warmer and drier climates. General circulation models still disagree in reproducing these changes and little has been done to derive them from first principles. Here, we present an alternative approach to describe the effects of tropical land conversion from forest to soy agriculture, based on a physical theory of land-atmosphere interactions. We view land-atmosphere exchange as the result of a heat engine strongly shaped by turbulent heat exchange. This provides a framework to derive analytical expressions of the turbulent fluxes from the limit by how much work this engine can maximally perform. By comparing these with observations from a tropical rainforest and a soybean field in Amazonia, we find that the diurnal variations of turbulent fluxes are very well estimated. This means that turbulent land-atmosphere exchange is primarily constrained by the thermodynamic limit, irrespective of surface roughness and evapotranspiration, and suggests that one can estimate the primary impacts of tropical land use change from physical principles. Thus, using thermodynamic limits represents an alternative approach to investigate the highly complex nature of land-atmosphere interactions and global change from first principles.

1. Introduction

Amazonian deforestation has surpassed 700 million km² and substantially changed the surface energy balance, with important implications for the local and regional climate (e.g., D'Almeida et al., 2007; Gash & Nobre, 1997; Lawrence & Vandecar, 2015; Nobre et al., 1991). As deep-rooted forests are converted into shallow-rooted crops and pasturelands, surface albedo increase (Gash & Shuttleworth, 1991), aerodynamic surface roughness decreases, and access to soil water becomes limited (Kleidon & Heimann, 2000; Nepstad et al., 1994). Because of these changes, deforested areas typically evaporate less and are much warmer (see, e.g., review by D'Almeida et al., 2007).

Although many land surface models can reproduce changes in the regional surface energy balance caused by Amazonian deforestation (Lawrence & Vandecar, 2015), there is still a major need to describe such changes from first principles. Filling this knowledge gap would reduce the need for complex numerical simulation models and provide methods to derive first-order approximations of deforestation-related effects on land surface functioning and the water budget. A major difficulty in doing so is that calculations of the turbulent heat fluxes in the surface energy balance seemingly depend on several meteorological variables, such as wind

speed, atmospheric stability, temperature, and moisture gradients. One approach to address this challenge is to use thermodynamic principles to constrain the magnitude of turbulent fluxes and thus provide an estimate of them.

To constrain turbulent heat fluxes using thermodynamics, we view these fluxes as both the driver and the result of an atmospheric heat engine operating between the warm surface and the cold atmosphere. Assuming that this engine operates at its thermodynamic limit, we can then constrain the magnitude of turbulent heat fluxes, yielding an analytic formulation of the surface energy balance. Previous applications of this thermodynamic framework were shown to provide reasonable estimates of the surface energy and water balance across different climates (Kleidon et al., 2014) and the sensitivities of the hydrological cycle and the land-ocean temperature contrast to global warming (Kleidon & Renner, 2013; Kleidon & Renner, 2017).

Here, we employ this thermodynamic approach to quantify differences in the surface energy balance between a tropical rainforest and a soybean field, one of the most common land uses in southeastern Amazonia. We use observations of the surface energy balance at two eddy flux sites at the Tanguro Ranch (Balch et al., 2008; Nagy et al., 2018; Silvério et al., 2013). We focus the evaluation particularly on the mean diurnal cycle during 1 month of the wet and dry season, respectively, using a recent extension of the thermodynamic approach that accounts for diurnal variations in the surface fluxes (Kleidon, 2016; Kleidon & Renner, 2018). We use observed solar radiation as the primary forcing and predict the turbulent heat fluxes, which we then compare to observed net radiation at both sites. We further test the extent to which variations in longwave emissivity of the atmosphere alter the estimates between the dry and the wet season, and evaluate how well the sensible and latent heat flux can be derived from the estimated turbulent heat flux. With this we aim to test how well this approach can capture surface energy balance partitioning for these very different tropical land cover types.

In the following, we first provide a brief description of the thermodynamic approach and an extension to a more detailed treatment of longwave radiation, and the observations we use at the two sites (details on experimental setting and theoretical derivations are provided in the supporting information). The analysis of the results focuses on the predicted diurnal cycles. We then evaluate the role of longwave radiation as well as differences in the greenhouse effect during wet and dry season on the predicted turbulent heat fluxes. The main effects of land cover change are then discussed in the context of previous studies. We close with an outlook on potential future extensions of the thermodynamic approach and the utility of the approach in understanding the climatic effects of land cover change.

2. Materials and Methods

2.1. Turbulent Fluxes From Thermodynamics

We estimate turbulent heat fluxes from the absorbed solar radiation at the surface (R_s) using a combination of the thermodynamic limit for a heat engine, the surface energy balance, a parameterization for longwave radiation, and the energy balance of the whole surface-atmosphere system (Kleidon, 2016; Kleidon & Renner, 2018). The thermodynamic limit is used to determine the maximum in mechanical power that can be derived from the turbulent heat fluxes ($J = H + LE$), that is, the sum of the sensible (H) and latent (LE) heat flux (with L being the latent heat of vaporization and E being evapotranspiration). The maximization requires an expression for surface temperature (T_s) as greater turbulent heat fluxes result in cooler surface temperatures. This relationship is obtained from the surface energy balance and a parameterization of longwave radiation at the surface. For the thermodynamic limit, we use a formulation that considers the strong diurnal variations of heat content in the lower atmosphere during the day (Kleidon & Renner, 2018).

The maximization of power yields the following analytic expression for the optimum turbulent heat flux in the surface energy balance:

$$J_{opt} = \frac{1}{2} \left(R_s - R_{l,0}(\tau) - \frac{dU_s}{dt} + \frac{dU_a}{dt} \right), \quad (1)$$

where R_s is the absorbed solar radiation at the surface, $R_{l,0}(\tau) = R_{l,toa} - R_{l,d}$ is a constant from the parameterization of net longwave radiation that decreases with the optical depth of the atmosphere, τ , $\frac{dU_s}{dt}$ is the

change in the surface heat storage, and $\frac{dU_a}{dt}$ is the heat storage change in the lower atmosphere (inferred from the daily variation of solar radiation). A more extensive treatment of the approach with derivation of equation (1) is provided in S1 of the supporting information.

We then infer the sensible and latent heat fluxes as in Kleidon et al. (2014) using the equilibrium partitioning (Penman, 1948; Priestley & Taylor, 1972; Schmidt, 1915)

$$H_{opt} = \frac{\gamma}{\gamma + s} J_{opt}, \quad (2)$$

$$LE_{opt} = \frac{s}{\gamma + s} J_{opt}, \quad (3)$$

where γ is the psychrometric constant and s is the slope of the saturation vapor pressure curve. Note that equation (3) describes conditions in which soil water availability does not limit evapotranspiration. To account for water limitation, we introduce a factor (f_w) to reduce the latent heat flux (with $0 \leq f_w \leq 1$) and then apply this correction to the partitioning: $LE_{opt,limit} = f_w LE_{opt}$ and $H_{opt,limit} = J_{opt} - LE_{opt,limit}$. We assume that the magnitude of turbulent fluxes, as set by the maximum power limit, is not affected, so $J_{opt,limit} = J_{opt}$.

2.2. Field Sites

We use observations from an intact broadleaf evergreen transitional rainforest between Amazonia and Cerrado and a soybean site at the southeastern Amazonian agricultural frontier, a region that experienced large-scale deforestation in the 1970s, with cattle pastures being converted to soybean fields since the early 2000s (Silvério et al., 2013). Data on energy and water fluxes come from two eddy covariance flux towers placed in intact forest and soybean fields roughly a kilometer apart. The towers are located at the Tanguro Ranch, Mato Grosso, Brazil (13°04'35.39"S, 52°23'08.85"W) at an elevation of 380 m above sea level. The mean annual temperature of the region is 25 °C and the annual precipitation is about 1,770 mm per year (Rocha et al., 2014). This region is subject to highly seasonal rainfall, with precipitation during the dry season being less than 10 mm per month from May to August. The soybeans are generally planted in October or November and harvested in March or April. During the noncropping season, fields were bare or had a sparse cover crop of millet. Further details on the sites are provided in Balch et al. (2008), Silvério et al. (2013), Nagy et al. (2018), and S2 of the supporting information.

2.3. Data Analysis

We focused our analysis on the mean diurnal cycle of 2 months of June 2016 (dry season) and January 2017 (wet season) at time intervals of 30 min. The estimate of the optimum turbulent heat flux (equation (1)) requires information about surface absorption of solar radiation (R_s , from which $\frac{dU_a}{dt}$ is derived, equation S5 in S1 of the supporting information), the ground heat flux ($\frac{dU_g}{dt}$) and the value of $R_{l,0}(\tau)$ derived from the parametrization of longwave radiative transfer. For the first two variables, we directly use the observed quantities. We estimate the value of $R_{l,0}(\tau)$, and τ , using an expression for the atmospheric emissivity from Brutsaert (1975) that depends on observations of near-surface air temperature (T_a) and water vapor pressure (e_a) (details in S1 of the supporting information). We set a value of $T_r = 268 \pm 17$ K (details in S2 of the supporting information). This parametrization of longwave radiation captures the seasonal variations in the greenhouse effect due to changes in emissivity (denoted as “derived optical thickness” estimate, see Table 1). For comparison, we also estimate the turbulent heat flux $J'_{opt} = \frac{1}{2} (R_s - \frac{dU_s}{dt} + \frac{dU_a}{dt})$ without variations in τ (i.e., $R_{l,0}(\tau) = 0$ with $\tau = 4/3$, denoted as “fixed optical thickness” estimate). A more extensive description of the parameterization of longwave radiation is provided in S1 of the supporting information.

To estimate the sensible and latent heat fluxes we use equations (2) and (3) with a value of $\gamma = 65 \text{ Pa K}^{-1}$. We derived the skin temperature from surface longwave emission ($R_{l,up}$), $T_s = \left(\frac{R_{l,up}}{\sigma}\right)^{\frac{1}{4}}$, and calculated the slope of the saturation vapor pressure curve, s , using the expression of Bohren and Albrecht (1998). We estimated the water limitation factor by comparing the observed latent heat flux, LE_{obs} , with the optimum latent heat flux (equation (3)), $f_w = LE_{obs}/LE_{opt}$ and applied this to our expressions as described above.

Table 1
Monthly Mean Forcing Variables for Each Site and Season

Forcing variables	Dry season (June 2016)		Wet season (January 2017)	
	Forest	Soybeans	Forest	Soybeans
Observed net shortwave absorption at the surface $R_{s,avg}(W/m^2)$	181 ± 51	192 ± 51	223 ± 46	227 ± 51
Observed 2 m-air temperature $T_a(K)$	301 ± 2	299 ± 1	300 ± 1	299 ± 1
Observed 2 m-air water vapor pressure $e_a(hPa)$	21 ± 4	20 ± 3	29 ± 1	29 ± 1
Derived long wave optical thickness τ	2.20 ± 0.10	2.13 ± 0.08	2.27 ± 0.04	2.25 ± 0.03
Estimated longwave downwelling radiation ^a $R_{l,d}(W/m^2)$	412 ± 20	395 ± 15	425 ± 6	421 ± 5
Observed longwave downwelling radiation $R_{l,d,obs}(W/m^2)$	389 ± 16	400 ± 13	414 ± 7	422 ± 5
Estimated longwave radiative cooling ^b $R_{l,toa}(W/m^2)$	292 ± 19			
Estimated radiation parameter $R_{l,o}(W/m^2)$ ^c	-110 ± 20	-93 ± 15	-124 ± 6	-119 ± 18
Estimated water limitation factor f_w ^d	1.3 ± 0.1	1.1 ± 0.2	0.2 ± 0.1	1.2 ± 0.1

^a $R_{l,d} = \frac{3}{4} \tau \sigma T_r^4$. ^b $R_{l,toa} = \sigma T_r^4$. ^c $R_{l,o} = R_{l,toa} - R_{l,d}$. Derivations in S1 of the supporting information. ^dEstimation in S2 of the supporting information.

We evaluated the agreement between the estimated and observed fluxes by means of ordinary least square regression. An ideal agreement is described by a correlation coefficient of $r^2 = 1$, a slope of 1 and an intercept of zero. We only consider daytime values of the fluxes in the statistics to avoid a nighttime bias when convection is not generated by buoyancy due to the lack of heating by solar radiation.

3. Results and Discussion

Overall, the turbulent heat fluxes estimated from our thermodynamic approach reproduce observations for the forest and soybean sites very well (see Figure 1 and Table 2). Figure 1 compares the mean diurnal

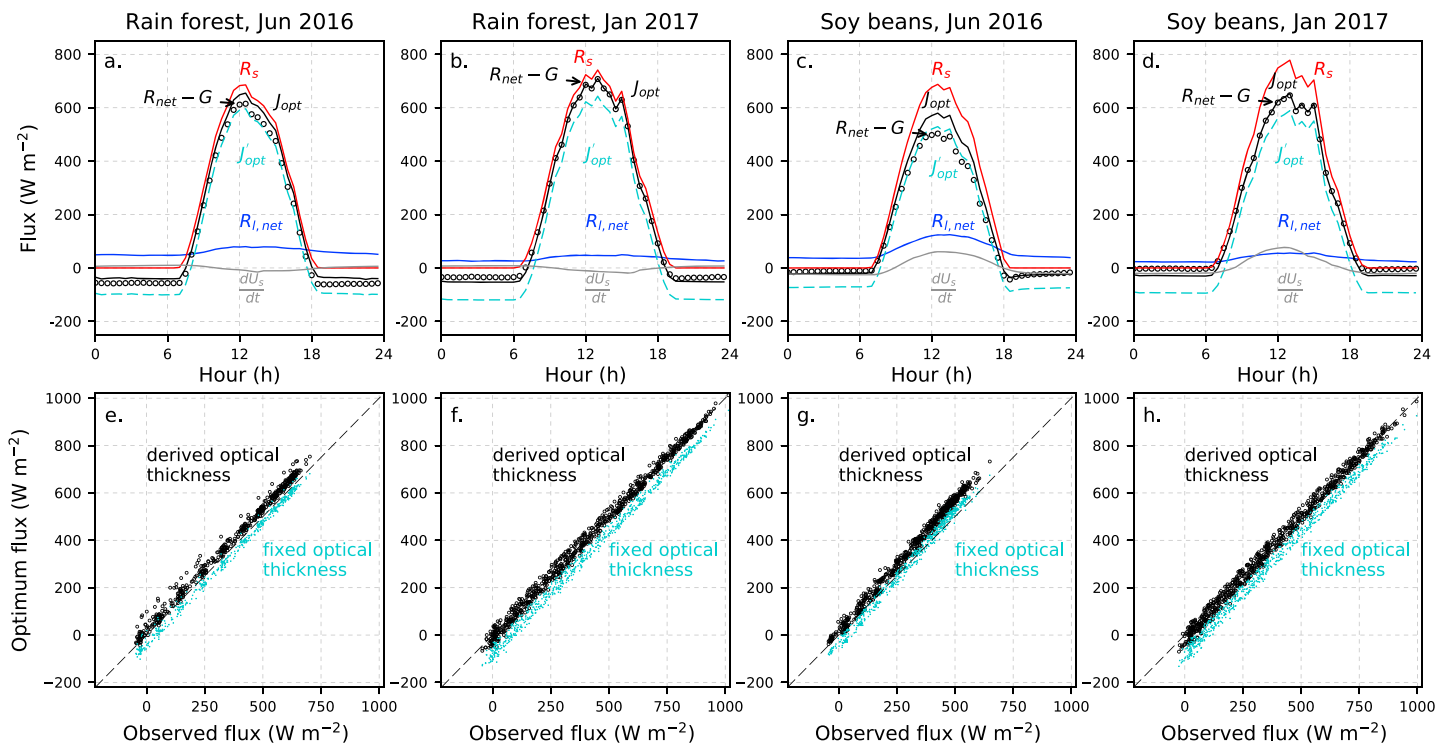


Figure 1. Estimated and observed surface energy balance partitioning for the rainforest and soybean sites for 1 month in the dry and wet season. The top row (a–d) shows the observations of the absorbed solar radiation at the surface (R_s , red), net long wave radiation ($R_{l,net}$, blue), the ground heat flux ($\frac{dU_s}{dt}$, gray), turbulent heat fluxes ($R_{net} - G$, circles), and the two estimates of turbulent heat fluxes from the maximum power limit with derived (J_{opt} , black) and fixed (J_{opt} , cyan) optical thicknesses. The bottom row (e–h) shows scatter plots between the estimated turbulent heat fluxes (J_{opt} , derived (black) and fixed (cyan)) against observations ($R_{net} - G$). Nighttime values are not shown in the scatterplots.

Table 2
Ordinary Least Squares Regression Statistics for the Turbulent Heat Fluxes

Turbulent heat fluxes	Dry season (June 2016)				Wet season (January 2017)			
	Intercept (W/m ²)	Slope (–)	r ² (–)	NRMSE (%)	Intercept (W/m ²)	Slope (–)	r ² (–)	NRMSE (%)
Forest								
Turbulent fluxes J'_{opt} (fixed optical thickness)	-34.02 ± 1.27	1.03 ± 0.01	0.99	2	-73.89 ± 1.14	1.01 ± 0.01	1.00	2
Turbulent fluxes J_{opt} (derived optical thickness)	26.30 ± 1.58	1.02 ± 0.01	0.99	2	-6.84 ± 1.23	1.01 ± 0.01	1.00	2
Latent heat flux LE_{opt}	-4.37 ± 5.96	0.97 ± 0.02	0.96	6	-19.06 ± 4.61	1.02 ± 0.01	0.98	4
Sensible heat flux H_{opt}	54.52 ± 2.97	0.57 ± 0.05	0.51	18	29.42 ± 3.46	0.70 ± 0.04	0.73	15
Soybeans								
Turbulent fluxes J'_{opt} (fixed optical thickness)	-38.42 ± 1.27	1.12 ± 0.01	0.99	2	-79.58 ± 1.14	1.03 ± 0.01	0.99	2
Turbulent fluxes J_{opt} (derived optical thickness)	13.20 ± 1.31	1.12 ± 0.01	0.99	2	-14.63 ± 1.36	1.03 ± 0.01	0.99	2
Latent heat flux LE_{opt}	32.97 ± 3.72	0.38 ± 0.05	0.32	23	-12.02 ± 4.64	0.96 ± 0.01	0.95	6
Sensible heat flux H_{opt}	17.61 ± 4.65	0.89 ± 0.02	0.94	7	34.38 ± 2.94	0.48 ± 0.04	0.37	19

Note. Statistics are computed from half-hourly, daytime values of the whole month. NRMSE = normalized root mean square error.

variation of the turbulent fluxes together with the other observed surface energy balance components. Correlation coefficients and slopes are generally close to one for both sites and seasons (Table 2). We find, however, that the turbulent heat flux is somewhat overestimated during the dry season for the soybean site by about 12%. This bias is likely to be related to the greater transparency of the atmosphere, which could be dealt with by a more detailed parameterization of radiative transfer. From this agreement we can nevertheless conclude that turbulent fluxes appear to operate near their thermodynamic limit and can be estimated from our approach.

Variations in the longwave optical depth affect primarily the intercept in the linear regression but do not alter the slope and correlation coefficient. The fixed optical thickness estimate results in offsets of about $33.5 - 38.8 \frac{W}{m^2}$ in the dry season and a greater offset of $73.9 - 79.6 \frac{W}{m^2}$ during the wet season (Table 2). This comparatively uniform offset can be understood directly by our expression for the optimum turbulent heat flux (equation (1)). There, the optical thickness affects $R_{l,0}(\tau)$ which adds a constant offset to J_{opt} that is independent of the instantaneous solar forcing. When the variations in atmospheric emissivity are accounted for using the parameterization of Brutsaert (1975) and by estimating the radiative temperature of the atmosphere, then the offsets are considerably reduced in magnitude to $13.20 - 26.30 \frac{W}{m^2}$ (dry season) and $-6.84 - -14.63 \frac{W}{m^2}$ (wet season), respectively. We find that in this parameterization, it is particularly the variation in water vapor pressure between June (about 20 hPa for both sites, Table 1) and January (about 29 hPa for both sites, Table 1) that accounts for most of this variation in optical thickness. What this implies is that although variations in longwave radiation affect the turbulent heat flux to some extent, their overall effect on diurnal variations is comparatively minor.

Figure 2 compares the sensible and latent heat fluxes derived from the optimum turbulent heat fluxes using equations (2) and (3) with observations. The agreement is, again, very good, except in few cases for the soybean site. Correlation coefficients are above 95% for the latent heat flux, and a somewhat poorer correlation for the sensible heat flux (Table 2). The slope of the latent heat flux is near one, while it appears that the sensible heat flux is somewhat underestimated. Water limitation only plays an important role during the dry season at the soybean site, with an estimated limitation factor $f_w \approx 0.2$ derived from observations (see S2 of the supporting information). The reduced latent heat flux is then compensated for by a higher sensible heat flux. For the rainforest site in both seasons and for the soybean site in the wet season, the estimated limitation factor is $f_w \approx 1$, so that water limitation did not play a major role in shaping the latent heat flux. This means that one of the major differences between the rainforest and soybean sites is soil water availability associated with deep-rooted tropical rainforests, an aspect that is well recognized to play an important role in land cover changes in Amazonia (e.g., Kleidon & Heimann, 2000; Nepstad et al., 1994). What our analysis also shows is that water availability change due to land cover change mainly affects the partitioning of turbulent heat fluxes into sensible and latent heat, but not the overall magnitude of turbulent heat fluxes that is

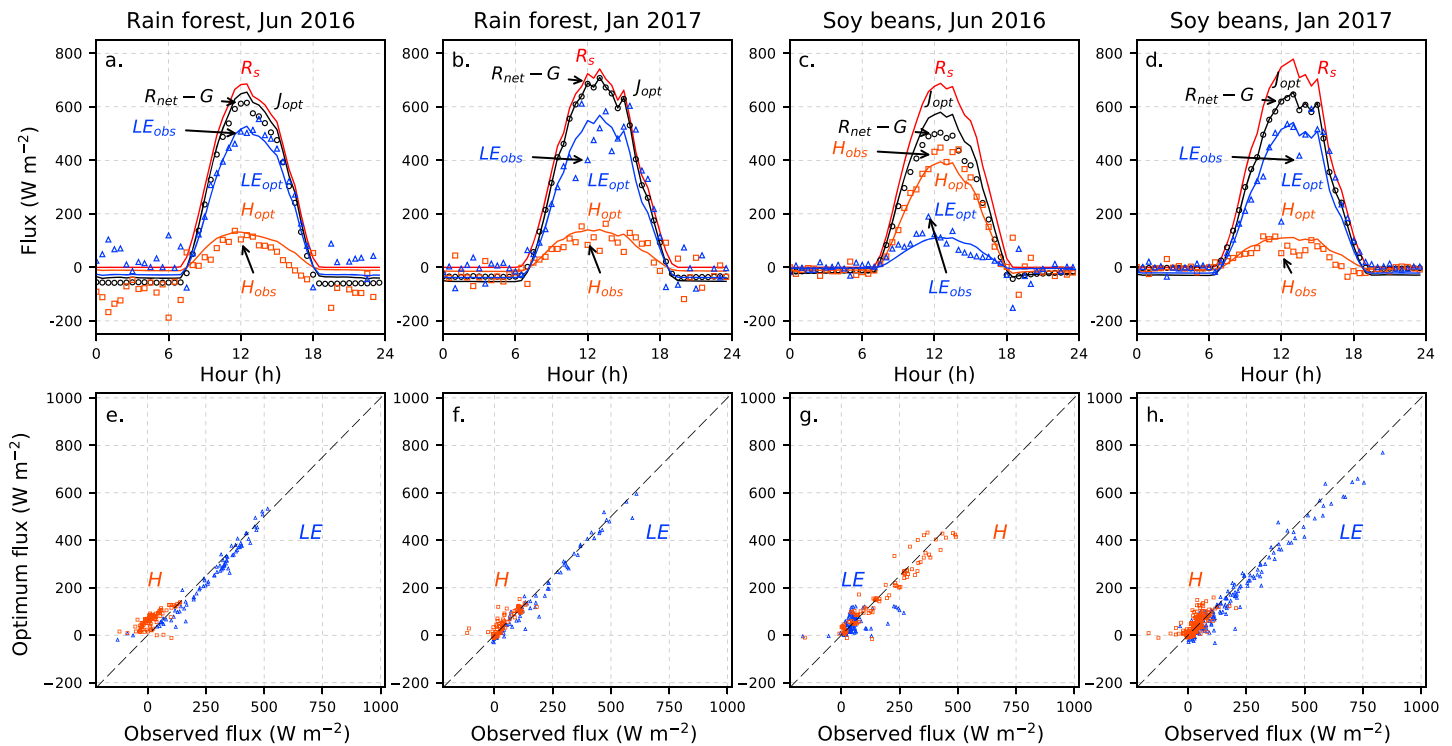


Figure 2. As Figure 1, but for the partitioning of the turbulent heat flux into sensible and latent heat. Shown are the turbulent heat flux (black, observations ($R_{net} - G$, circles) and estimated (J_{opt} , line)), the sensible (light red, observations (H_{obs} , squares) and estimated (H_{opt} , line)), and latent heat flux (blue, observations (LE_{obs} , triangles) and estimated (LE_{opt} , line)). For reference, absorbed solar radiation (R_s) is shown by the red line. The bottom row (e–h) shows scatter plots between observed and estimated fluxes of sensible (H , red) and latent heat (LE , blue). Nighttime values are not shown in the scatterplot.

set by the thermodynamic maximum power limit. A somewhat surprising implication of this finding is that the substantial difference in surface roughness between the tropical rainforest and soybean sites apparently has little effect on the magnitude of the turbulent heat fluxes and their partitioning.

While our approach captures the overall differences in surface energy balance partitioning between forest and cropland sites, it has some limitations. First, we are not yet able to infer changes in surface and air temperatures from our approach. To accomplish this, one would need to explicitly link the heat storage variations in the lower atmosphere to boundary layer dynamics and to air temperature variations. This, however, would require additional work. Second, our approach does not apply to the stable nighttime conditions when the absence of surface heating does not generate buoyancy and convection. Currently, our approach does not consider atmospheric stability explicitly, which could in principle be inferred from surface and air temperatures. Third, we do not account for irreversible losses associated with evaporation and other transient effects that affect the power available for convection. Dissipation due to the evaporation into unsaturated air reduces the total power available for turbulent exchange and this may alter the outcome of the maximization. In principle, a fully thermodynamic description of the soil-vegetation-atmosphere system would help to overcome these limitations. Addressing these aspects would certainly improve model predictions and have the potential to infer more variables and aspects of land-atmosphere dynamics from first principles. Yet, the high explained variance of our simple expression for the turbulent heat flux (equation (1)) and its partitioning (equations (2) and (3)) suggests that these capture the basic physical factors shaping turbulent land-atmosphere exchange and can provide relevant insights into the dominant changes associated with tropical deforestation.

Changes in surface energy balance partitioning associated with tropical deforestation have been evaluated thoroughly over the years based on both observations and different modeling approaches (e.g., reviews by D'Almeida et al., 2007; Lawrence & Vandecar, 2015). We advance this understanding of land surface processes by showing that the magnitude of turbulent heat fluxes of the two sites are shaped primarily by the absorption of solar radiation and the thermodynamic limit. Our formulation (equation (1)) can explain

turbulent fluxes at both sites and seasons, regardless of the highly contrasting land cover of the two sites. The changes in longwave optical thickness during the dry and wet season have a comparatively minor effect on this partitioning and merely alters the offsets in Figure 1, as shown in the correlation statistics in Table 2.

The equilibrium partitioning into sensible and latent heat then works well during the wet season, but for the dry season, it shows the dominant role of water limitation for the soybean site due to the lack of vegetative cover and access to soil water storage. The main difference in surface energy balance partitioning of the two sites are then primarily the presence of water limitation during the dry season at the soybean site, apart from differences in the absorption of solar radiation and soil heat fluxes. This water limitation resulted in a reduction in evapotranspiration of $\frac{LE}{LE} \approx \frac{A_{f,w}}{f_w} \approx 80\%$ during the dry season, noting that the difference in turbulent heat fluxes is small. To evaluate this impact of land cover change more generally would require a soil water balance model to simulate the seasonal course of the reduction factor f_w .

What is somewhat surprising in these results is that the difference in surface roughness between the sites seems to play only a small role in shaping the magnitude of turbulent fluxes. This likely suggests that the dominant driver of land surface-atmosphere exchange at these sites is surface heating by the absorption of solar radiation. This heating generates buoyancy and the associated fluxes of sensible and latent heat. Our thermodynamic limit then sets the magnitude of the buoyancy flux, which is why the surface energy balance partitioning can be explained so well by the combination of absorbed solar radiation and the thermodynamic limit without knowing the wind conditions.

4. Conclusions

We showed that the turbulent heat flux of the surface energy balance across two different types of land cover in southeastern Amazonia can be estimated very well from the maximum power principle. This provides a novel, parameter-sparse approach to estimate the effects of land cover change that can be used to benchmark the performance of climate model simulations. The maximum in power is set by thermodynamics, a surface energy balance trade-off by which a greater turbulent flux leads to a lower surface temperature, and by diurnal heat storage variations in the lower atmosphere. Our results show that the major effects of tropical deforestation on the surface energy balance are changes in how much solar radiation is absorbed and changes in water limitation at the non-forested site. The turbulent heat flux was estimated very well by the maximum power limit at both sites, suggesting that the turbulent heat flux over land operates at its thermodynamic limit irrespective of water availability and differences in surface roughness.

What we conclude from this is that our approach represents an adequate basis to understand the first-order effects of land cover change. It yields a novel perspective on land-atmosphere interactions at the diurnal scale and how these are affected by land cover change. These interactions are reflected in our approach at a basic level. It is the buffering of the strong diurnal variation of solar radiation by heat storage changes in the lower atmosphere that intimately links the functioning of the land surface to the lower atmosphere, yet with its magnitude well constrained by the energy balance of the surface-atmosphere system. This buffering then affects the thermodynamic limit quite substantially. What our results then indicate is that land-atmosphere exchange at the diurnal scale is thus predominantly constrained by this heat buffering and the thermodynamic limit of how much work can be derived from the solar radiative heating. This constraint does not change with land cover change, while the partitioning of turbulent fluxes into sensible and latent heat is strongly affected by the land cover.

References

- Balch, J. K., Nepstad, D. C., Brando, P. M., Curran, L. M., Portela, O., De Carvalho, O., & Lefebvre, P. (2008). Negative fire feedback in a transitional forest of southeastern Amazonia. *Global Change Biology*, *14*, 2276–2287. <https://doi.org/10.1111/j.1365-2486.2008.01655.x>
- Bohren, C. F., & Albrecht, B. A. (1998). *Atmospheric thermodynamics*. New York: Oxford University Press.
- Brutsaert, W. (1975). On a derivable formula for long-wave radiation from clear skies. *Water Resources Research*, *11*(5), 742–744. <https://doi.org/10.1029/WR011i005p00742>
- D'Almeida, C., Vörösmarty, C. J., Hurr, G. C., Marengo, J. A., Dingman, S. L., & Keim, B. D. (2007). The effects of deforestation on the hydrologic cycle in Amazonia: A review on scale and resolution. *International Journal of Climatology*, *27*, 633–647. <https://doi.org/10.1002/joc.1475>
- Gash, J. H. C., & Nobre, C. A. (1997). Climatic effects of Amazonian deforestation: Some results from ABRACOS. *Bulletin of the American Meteorological Society*, *78*, 823–830. [https://doi.org/10.1175/1520-0477\(1997\)078<0823:CEOADS>2.0.CO;2](https://doi.org/10.1175/1520-0477(1997)078<0823:CEOADS>2.0.CO;2)

Acknowledgments

We thank Hisashi Ozawa and an anonymous reviewer for valuable comments and discussion. This work resulted from an internship of LC in the Biospheric Theory and Modeling group. LC acknowledges this internship and funding from the “Torno Subito” 2017 project of the Lazio Region (Italy) co-funded by the European Social Fund (FSE) 2014-2020 to support research on this study. This research contributes to the “Catchments As Organized Systems (CAOS)” research group (FOR 1598) funded by the German Science Foundation (DFG). P. B. received support from the National Science Foundation (#1802754) and from the Conselho Nacional de Desenvolvimento Científico e Tecnológico (CNPq-Brazil) through a Productivity grant PELD-Tang (#441703/2016-3). CNPq also supported S. T. through a PVE-Science without Borders (#405800/2013-4). S. T. and P. B. thank the EU, the German Bundesanstalt für Landwirtschaft und Ernährung FKZ: 2816ERA03W (to S. T.), and the International Development Research Centre of Canada (Project ID 10850, to P. B.) for funding, in the frame of the collaborative international Consortium AgWIT financed under the ERA-NET WaterWorks2015 Cofunded Call. This ERA-NET is an integral part of the 2016 Joint Activities developed by the Water Challenges for a Changing World Joint Programme Initiative (Water JPI). All the data used in the analysis are available online (at <https://doi.org/10.5281/zenodo.2575711>).

- Gash, J. H. C., & Shuttleworth, W. J. (1991). Tropical deforestation: Albedo and the surface-energy balance. *Climatic Change*, *19*, 123–133. <https://doi.org/10.1007/BF00142219>
- Kleidon, A. (2016). *Thermodynamic foundation of the Earth system*. Cambridge: Cambridge University Press. <https://doi.org/10.1017/CBO9781139342742>
- Kleidon, A., & Heimann, M. (2000). Assessing the role of deep rooted vegetation in the climate system with model simulations: Mechanism, comparison to observations and implications for Amazonian deforestation. *Climate Dynamics*, *16*, 183–199. <https://doi.org/10.1007/s003820050012>
- Kleidon, A., & Renner, M. (2013). A simple explanation for the sensitivity of the hydrologic cycle to climate change. *Earth System Dynamics*, *4*(2), 455–465. <https://doi.org/10.5194/esd-4-455-2013>
- Kleidon, A., & Renner, M. (2017). An explanation for the different climate sensitivities of land and ocean surfaces based on the diurnal cycle. *Earth System Dynamics*, *8*, 849–864. <https://doi.org/10.5194/esd-8-849-2017>
- Kleidon, A., & Renner, M. (2018). Diurnal land surface energy balance partitioning estimated from the thermodynamic limit of a cold heat engine. *Earth System Dynamics*, *9*, 1127–1140. <https://doi.org/10.5194/esd-9-1127-2018>
- Kleidon, A., Renner, M., & Porada, P. (2014). Estimates of the climatological land surface energy and water balance derived from maximum convective power. *Hydrology and Earth System Sciences*, *18*, 2201–2218. <https://doi.org/10.5194/hess-18-2201-2014>
- Lawrence, D., & VandeCar, K. (2015). Effects of tropical deforestation on climate and agriculture. *Nature Climate Change*, *5*, 27–36. <https://doi.org/10.1038/NCLIMATE2430>
- Nagy, R. C., Porder, S., Brando, P., Davidson, E. A., Figueira, A. M. e. S., Neill, C., et al. (2018). Soil carbon dynamics in soybean cropland and forests in Mato Grosso, Brazil. *Journal of Geophysical Research: Biogeosciences*, *123*, 18–31. <https://doi.org/10.1002/2017JG004269>
- Nepstad, D. C., de Carvalho, C. R., Davidson, E. A., Jipp, P. H., Lefebvre, P. A., Negreiros, G. H., et al. (1994). The role of deep roots in the hydrological and carbon cycles of Amazonian forests and pastures. *Nature*, *372*, 666–669. <https://doi.org/10.1038/372666a0>
- Nobre, C. A., Sellers, P. J., & Shukla, J. (1991). Amazonian deforestation and regional climate change. *Journal of Climate*, *4*, 957–988. [https://doi.org/10.1175/1520-0442\(1991\)004<0957:ADARCC>2.0.CO;2](https://doi.org/10.1175/1520-0442(1991)004<0957:ADARCC>2.0.CO;2)
- Penman, H. L. (1948). Natural evaporation from open water, bare soil, and grass. *Proceedings of the Royal Society of London A*, *193*, 120–146.
- Priestley, C. H. B., & Taylor, R. J. (1972). On the assessment of surface heat flux and evaporation using large-scale parameters. *Monthly Weather Review*, *100*, 81–92. [https://doi.org/10.1175/1520-0493\(1972\)100<0081:OTAOSH>2.3.CO;2](https://doi.org/10.1175/1520-0493(1972)100<0081:OTAOSH>2.3.CO;2)
- Rocha, W., Metcalfe, D. B., Doughty, C. E., Brando, P., Silvério, D., Halladay, K., et al. (2014). Ecosystem productivity and carbon cycling in intact and annually burnt forest at the dry southern limit of the Amazon rainforest (Mato Grosso, Brazil). *Plant Ecology and Diversity*, *7*(1–2), 25–40. <https://doi.org/10.1080/17550874.2013.798368>
- Schmidt, W. (1915). Strahlung und Verdunstung an freien Wasserflaechen; ein Beitrag zum Waermehaushalt des Weltmeeres und zum Wasserhaushalt der Erde. *Ann. Calender Hydrographie und Maritimen Meteorologie*, *43*, 111–178.
- Silvério, D. V., Brando, P. M., Balch, J. K., Putz, F. E., Nepstad, D. C., Oliveira-Santos, C., & Bustamante, M. M. C. (2013). Testing the Amazon savannization hypothesis: Fire effects on invasion of a neotropical forest by native cerrado and exotic pasture grasses. *Philosophical Transactions of the Royal Society B*, *368*, 20120427. <https://doi.org/10.1098/rstb.2012.0427>

References From the Supporting Information

- Aubinet, M., Vesala, T., & Papale, D. (2012). *Eddy covariance: A practical guide to measurement and data analysis*. London, New York: Springer Atmospheric Sciences. <https://doi.org/10.1007/978-94-007-2351-14>
- Crawford, T. M., & Duchon, C. E. (1999). An improved parameterization for estimating effective atmospheric emissivity for use in calculating daytime downwelling longwave radiation. *Journal of Applied Meteorology*, *38*(4), 474–480. [https://doi.org/10.1175/1520-0450\(1999\)038<0474:AIPFEE>2.0.CO;2](https://doi.org/10.1175/1520-0450(1999)038<0474:AIPFEE>2.0.CO;2)
- Dhara, C., Renner, M., & Kleidon, A. (2016). Broad climatological variation of surface energy balance partitioning across land and ocean predicted from the maximum power limit. *Geophysical Research Letters*, *43*, 7686–7693. <https://doi.org/10.1002/2016GL070323>
- Foken, T. (2008). The energy balance closure problem—An overview. *Ecological Applications*, *18*, 1351–1367. <https://doi.org/10.1890/06-0922.1>
- Foken, T., & Wichura, B. (1996). Tools for quality assessment of surface-based flux measurements. *Agricultural and Forest Meteorology*, *78*(1–2), 83–105. [https://doi.org/10.1016/0168-1923\(95\)02248-1](https://doi.org/10.1016/0168-1923(95)02248-1)
- Goody, R. M., & Yung, Y. L. (1989). *Atmospheric radiation: Theoretical basis*. Oxford: Oxford University Press.
- Ozawa, H., Ohmura, A., Lorenz, R. D., & Pujol, T. (2003). The second law of thermodynamics and the global climate system—A review of the maximum entropy production principle. *Reviews of Geophysics*, *41*(4), 1018. <https://doi.org/10.1029/2002RG000113>
- Renno, N. O., & Ingersoll, A. P. (1996). Natural convection as a heat engine: A theory for CAPE. *Journal of the Atmospheric Sciences*, *53*, 572–585. [https://doi.org/10.1175/1520-0469\(1996\)053<0572:NCAAHE>2.0.CO;2](https://doi.org/10.1175/1520-0469(1996)053<0572:NCAAHE>2.0.CO;2)
- Twine, T. E., Kustas, W. P., Norman, J. M., Cook, D. R., Houser, P. R., Meyers, T. P., et al. (2000). Correcting eddy-covariance flux underestimates over a grassland. *Agricultural and Forest Meteorology*, *103*(3), 279–300. [https://doi.org/10.1016/S0168-1923\(00\)00123-4](https://doi.org/10.1016/S0168-1923(00)00123-4)
- Vickers, D., & Mahrt, L. (1997). Quality control and flux sampling problems for tower and aircraft data. *Journal of Atmospheric and Oceanic Technology*, *14*, 512–526. [https://doi.org/10.1175/1520-0426\(1997\)014<0512:QCAFSP>2.0.CO;2](https://doi.org/10.1175/1520-0426(1997)014<0512:QCAFSP>2.0.CO;2)